





Controlled release of dexamethasone phosphate from modified mesoporous biocompatible silica nanoparticles: synthesis, characterization, and kinetic studies

Juan Manuel Galdopórpora¹, María Victoria Olivera², Angelina Ibar³, Darío Hernán Farriol³, Martín Federico Desimone^{4,5}, Cynthia Melisa Melián Queirolo^{5,6}, Helena Pardo⁷ , María Victoria Tuttolomondo^{4,5*} 

¹Unidad de Investigación en Bioquímica Traslacional y Metabolismo (UBiTyM), Facultad de Odontología, Universidad de Buenos Aires, CABA 1113, Argentina

²Universidad Nacional de Quilmes, Quilmes 1876, Argentina

³Facultad de Farmacia y Bioquímica, Universidad de Buenos Aires, CABA 1113, Argentina

⁴Departamento de Ciencias Químicas, Facultad de Farmacia y Bioquímica, Universidad de Buenos Aires, CABA 1113, Argentina

⁵Instituto de Química y Metabolismo del Fármaco (IQUIMEFA), CONICET - Universidad de Buenos Aires, CABA 1113, Argentina

⁶Departamento de Sanidad, Nutrición, Bromatología y Toxicología, Facultad de Farmacia y Bioquímica, Universidad de Buenos Aires, CABA 1113, Argentina

⁷Centro NanoMat, Polo Tecnológico de Pando, Facultad de Química, Universidad de la República, Pando 15600, Uruguay

***Correspondence:** María Victoria Tuttolomondo, Departamento de Ciencias Químicas, Facultad de Farmacia y Bioquímica, Universidad de Buenos Aires, CABA 1113, Argentina; Instituto de Química y Metabolismo del Fármaco (IQUIMEFA), CONICET - Universidad de Buenos Aires, CABA 1113, Argentina. mv_tuttolomondo@ffyb.uba.ar mvtuttolomondo@gmail.com

Academic Editor: Xiqun Jiang, Nanjing University, China

Received: December 17, 2024 **Accepted:** February 11, 2025 **Published:** February 28, 2025

Cite this article: Galdopórpora JM, Olivera MV, Ibar A, Farriol DH, Desimone MF, Queirolo CMM, et al. Controlled release of dexamethasone phosphate from modified mesoporous biocompatible silica nanoparticles: synthesis, characterization, and kinetic studies. *Explor Drug Sci.* 2025;3: 100895. <https://doi.org/10.37349/eds.2025.100895>

Abstract

Aim: This study evaluates the efficacy of amino-functionalized mesoporous silica nanoparticles (MSNs) in the controlled release of dexamethasone phosphate (DexaP), aiming to enhance therapeutic outcomes and minimize systemic toxicity.

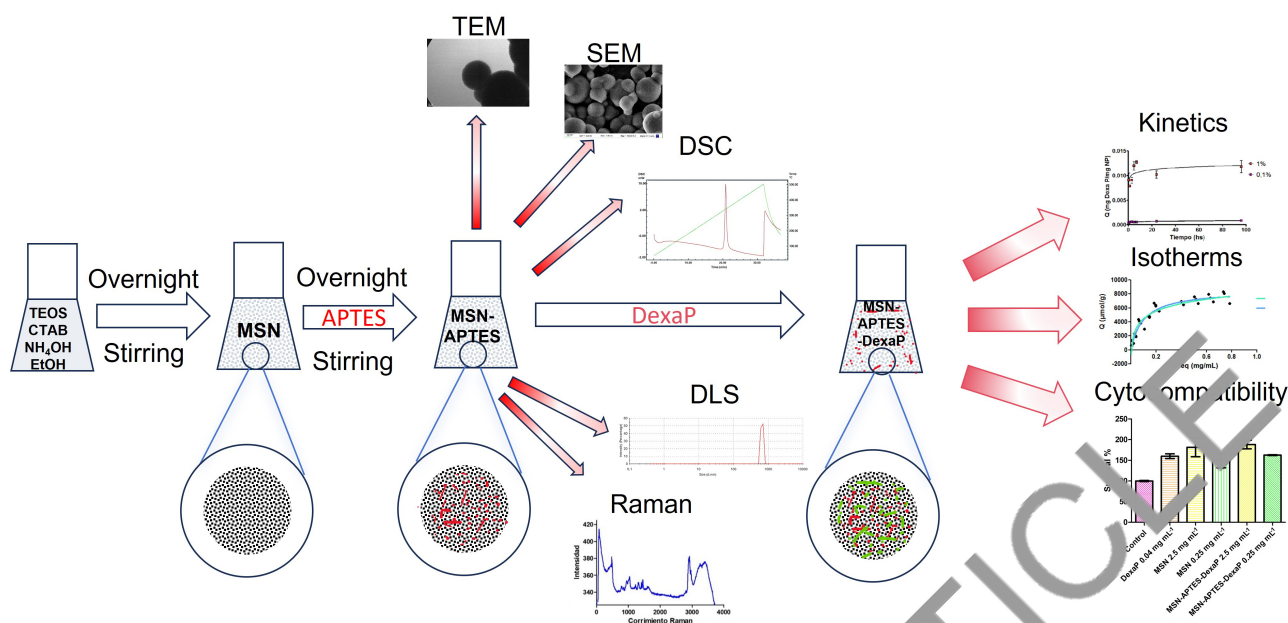
Methods: In this study, amino-functionalized MSNs were synthesized using a modified Stöber process and characterized their chemical and physical properties through various analytical techniques. The study focused on the adsorption and release kinetics of DexaP, employing multiple kinetic models to explore the interaction dynamics.

Results: The amino-functionalized MSNs demonstrated effective DexaP loading and controlled release profile. The kinetic analysis revealed a predominance of chemisorptive interactions, supporting sustained drug release. Enhanced biocompatibility was confirmed through cytotoxicity assays.

Conclusions: Amino-functionalized MSNs offer a promising platform for the targeted and controlled delivery of anti-inflammatory drugs, with significant potential to improve patient adherence and reduce adverse effects. The findings advocate for further development of MSNs as a versatile tool in advanced drug delivery systems.

© The Author(s) 2025. This is an Open Access article licensed under a Creative Commons Attribution 4.0 International License (<https://creativecommons.org/licenses/by/4.0/>), which permits unrestricted use, sharing, adaptation, distribution and reproduction in any medium or format, for any purpose, even commercially, as long as you give appropriate credit to the original author(s) and the source, provide a link to the Creative Commons license, and indicate if changes were made.





Graphical abstract. Amino-functionalized MSNs for the controlled adsorption and release of DexaP. TEOS: tetraethyl orthosilicate; CTAB: cetyltrimethylammonium bromide; EtOH: ethanol; MSN: mesoporous silica nanoparticle; APTES: 3-aminopropyltriethoxysilane; TEM: transmission electron microscope; SEM: scanning electron microscope; DSC: differential scanning calorimetry; DexaP: dexamethasone phosphate; DLS: dynamic light scattering.

Keywords

Drug delivery, dexamethasone, mesoporous, silica nanoparticles, controlled release, kinetics

Introduction

The development of nanotechnology has opened transformative pathways in drug delivery, especially for achieving controlled and targeted release of therapeutic agents [1, 2]. Mesoporous silica nanoparticles (MSNs) have gained significant attention in biomedical research due to their high surface area, tunable pore sizes, biocompatibility, and ability to be functionalized with diverse chemical groups [3]. These unique properties allow MSNs to encapsulate a wide range of therapeutic agents, including small molecules, proteins, and nucleic acids, making them especially suitable for biomedical applications. Their versatility is particularly promising for the delivery of anti-inflammatory drugs, such as dexamethasone phosphate (DexaP), where sustained release is essential to achieving prolonged therapeutic effects and reducing systemic toxicity [4].

DexaP is a potent anti-inflammatory and immunosuppressant drug widely used to treat conditions such as arthritis, allergic reactions, and respiratory distress. However, its clinical application is hampered by its short half-life and rapid systemic clearance, necessitating frequent administration that can reduce patient compliance and increase the risk of side effects [5, 6]. Encapsulation within MSNs offers a controlled release mechanism, overcoming these limitations by extending drug retention time and improving therapeutic outcomes. Additionally, this strategy reduces dosing frequency and enhances patient adherence to treatment regimens, offering significant benefits in chronic disease management [4].

In recent years, significant advancements have been made in the application of MSNs for drug delivery, as demonstrated by several studies, including those by Djayanti et al. [4] and Kim et al. [7]. These studies have explored the encapsulation and sustained release of various drugs using MSNs. Building upon this foundation, our work focuses specifically on the functionalization of MSNs with amino groups for enhanced interaction with DexaP, while also providing a detailed kinetic and thermodynamic analysis to better understand the release mechanisms. Unlike prior studies, our research emphasizes the biphasic release behavior and biocompatibility of functionalized MSNs, demonstrating their suitability for advanced drug delivery applications.

The functionalization of MSNs plays a critical role in optimizing their drug-loading capacity and release kinetics. Amino-functionalization using compounds such as 3-aminopropyltriethoxysilane (APTES) introduces positively charged amine groups onto the MSN surface. These groups enhance electrostatic interactions with negatively charged drug molecules, such as DexaP, resulting in improved drug loading and sustained release profiles [8–10]. Moreover, such modifications enable precise tuning of drug release rates, making MSNs highly adaptable to the therapeutic needs of different diseases [11, 12].

MSNs also exhibit high stability and biocompatibility, essential properties for safe and effective in vivo applications [13]. Their physicochemical properties, such as particle size, morphology, and surface charge, directly influence their performance as drug delivery systems [12]. Notably, zeta potential, a measure of nanoparticle surface charge, is a key parameter for ensuring stability in biological environments. High zeta potential prevents particle aggregation and promotes uniform dispersion, factors that are critical for maintaining drug delivery efficiency [14, 15].

This study aims to develop and evaluate amino-functionalized MSNs as a platform for DexaP delivery. We hypothesize that these modified MSNs will demonstrate effective drug loading, controlled release, and high biocompatibility. The findings from this work are expected to contribute to the advancement of drug delivery technologies, offering targeted, sustained release systems that minimize side effects and improve patient outcomes in the treatment of chronic inflammatory conditions.

Materials and methods

Synthesis of MSNs

MSNs were synthesized using a modified Stöber process [10], where 450 μ L of tetraethyl orthosilicate (TEOS; item NO.: 86578, Sigma-Aldrich) was added to a solution containing 3.85 mL deionized water, 6.3 mL absolute ethanol (item NO.: 2000165400, Biopack), 1.4 mL ammonia (item NO.: 1124110, Cicarelli), and 0.21 g cetyltrimethylammonium bromide (CTAB; item NO.: 52365, Sigma-Aldrich) as a template agent. After overnight agitation at 25°C, the nanoparticles were centrifuged at 25,000 G for 2 min at room temperature and thoroughly washed three times with anhydrous ethanol, three times with water, and then subjected to mineralization with a 9:1 $H_2O_3:H_2O$ mixture in a microwave digester to remove the CTAB template. Once mineralized, MSNs were thoroughly washed five times with distilled water, air dried at 25°C, and stored at room temperature in the dark until used.

Functionalization with amino groups

APTES (item NO.: 440140, Sigma-Aldrich) was used to introduce amino groups onto the MSN surface [9, 16]. Each 25 mg of MSN was dispersed in 10 mL anhydrous ethanol and 10 μ L APTES was added, followed by overnight agitation at 25°C. The modified nanoparticles were then centrifuged at 25,000 G for 2 min at room temperature, washed three times with anhydrous ethanol, and air dried at 25°C. The particles were then stored at room temperature in the dark until needed.

Characterization

The morphology and particle size were characterized using a scanning electron microscope (SEM, Zeiss SUPRA 40 microscope, Zeiss, Heidenheim an der Brenz, Germany) and a transmission electron microscope (TEM) at room temperature using a JEOL 1011 electron microscope (JEOL, Ltd. Tokyo, Japan), while particle size distribution and surface charge (zeta potential) were determined via dynamic light scattering (DLS) using a Nano-ZS (Zetasizer NanoZS, Malvern Instruments Ltd., Malvern, England). The surface chemistry changes were confirmed through a Raman confocal spectrometer WITec Alpha 300-R (Oxford Instruments WITec, Germany) with a 532 nm laser and a Shimadzu DSC-60 (Shimadzu Corporation, Kyoto, Japan) for differential scanning calorimetry (DSC).

Nanoparticles, both derivatized and non-derivatized, were stored for durations ranging from one week to one year post-synthesis without any observable differences in behavior. Stability was assessed through characterization prior to their use. The storage conditions were maintained at 25°C in the dark, without

humidity control. Similarly, DexaP-loaded nanoparticles were analyzed over a one-year period following their loading. All assays performed during this timeframe yielded consistent results, indicating no significant changes in behavior. These loaded nanoparticles were stored under the same conditions of 25°C in the dark, without humidity control.

Kinetics and thermodynamic modeling of dexamethasone adsorption and release

The kinetics and thermodynamics of DexaP uptake and release from amino-functionalized MSNs were evaluated at three different temperatures (4°C, 25°C, and 37°C) to investigate the impact of temperature on release mechanisms. Multiple kinetic models were applied, and thermodynamic parameters were calculated to understand the nature of the release process.

Adsorption kinetics

The experiment was carried out using two concentrations of DexaP. The experimental data were fitted to the following non-linear kinetic models [17].

Pseudo-first-order model

This model primarily describes systems where desorption from the particle surface is the controlling mechanism.

$$q_t = q_e(1 - e^{-k_1 t}) \quad (1)$$

where q_t is the amount of DexaP adsorbed at time t , q_e is the amount of DexaP adsorbed at equilibrium, k_1 is the pseudo-first-order adsorption constant and t is time. A poor fit for this model indicates significant contributions from other processes like diffusion or interactions with the particle matrix [18].

Pseudo-second-order model

A strong fit to this model indicates chemisorptive interactions between DexaP molecules and the amino-functionalized surface of the MSNs:

$$q_t = \frac{q_e^2 k_2 t}{1 + q_e k_2 t} \quad (2)$$

where k_2 is the pseudo-second-order rate constant [18].

Elovich model

This equation assumes that the adsorption sites of the sorbent are heterogeneous and therefore exhibit different activation energies for chemisorption.

$$q_t = \frac{1}{\beta \ln(1 + \alpha \beta t)} \quad (3)$$

where α is the initial adsorption rate and β relates to the amount of surface area covered and the activation energy involved in the chemisorption process (g mg^{-1}).

Adsorption isotherms

The adsorption and release of DexaP from MSNs were evaluated using Langmuir, Freundlich, Dubinin-Radushkevich (D-R), and Temkin isotherms. These models provide insight into the nature of interactions between DexaP and the MSN surface, as well as the adsorption mechanisms involved [17].

Langmuir isotherm

The Langmuir isotherm assumes monolayer adsorption at homogeneous binding sites [19] and is expressed as:

$$q_e = \frac{q_m K_a C_e}{1 + K_a C_e} \quad (4)$$

where q_e is the amount of DexaP adsorbed, q_m is the maximum adsorption capacity, K_a is the Langmuir constant, and C_e is the equilibrium concentration of DexaP.

Freundlich isotherm

The Freundlich isotherm describes heterogeneous adsorption [20] and is represented by:

$$q_e = K_F C_e^{1/n} \quad (5)$$

where K_F is the adsorption capacity constant, and n is the heterogeneity factor.

Dubinin-Radushkevich isotherm

The D-R model is used to describe physical adsorption [21] and is given by:

$$q_e = q_{DR} \exp(-\beta \epsilon^2) \quad (6)$$

where β is the adsorption energy constant, and ϵ is the Polanyi potential:

$$\epsilon = RT \ln\left(1 + \frac{1}{C_e}\right) \quad (7)$$

Temkin isotherm

The Temkin model assumes that the heat of adsorption decreases linearly with increasing surface coverage [22] and is expressed as:

$$q_e = \frac{RT}{b \ln(K_T C_e)} \quad (8)$$

where b is the Temkin constant related to adsorption energy, K_T is the equilibrium binding constant, R is the universal gas constant ($8.314 \text{ J mol}^{-1} \text{ K}^{-1}$) and T is the absolute temperature.

Release kinetic models

The release kinetics were analyzed using the following models.

Zero order

This is a widely used model for drug systems that do not disaggregate, making drug release very slow. For this model, it is assumed that the nanoparticle area does not change considerably and that material equilibrium conditions are not reached [23]. This is expressed from the following equation:

$$Q_t = Q_0 + k_0 t \quad (9)$$

where Q_t is the amount of drug dissolved (μg) at time t (h), Q_0 is the amount of initial drug in the solution (μg ; most of the time $Q_0 = 0$) and k_0 corresponds to the zero-order release constant.

First order

This model is used to describe the absorption and release of some drugs from porous matrices [24]. The release of drugs that follow these kinetics can be expressed by the equation:

$$\log C_t = \log C_0 - \left(\frac{k_1}{2.303}\right)t \quad (10)$$

where C_t is the amount of drug remaining (μg) at time t (h), C_0 is the initial amount of drug in the solution (μg) and k_1 is the first-order release constant.

As the amount of adsorbed drug decreases, the concentration of the dissolution medium becomes enriched with solute, so the release process is conditioned by the saturation point of the solute.

Higuchi model

The Higuchi model describes drug release driven by Fickian diffusion through a porous matrix:

$$q_t = k_H t^{1/2} \quad (11)$$

where k_H is the Higuchi constant related to the diffusional release rate. This model is widely applied for porous carriers like MSNs and is particularly relevant when the release is governed by diffusion [25].

Korsmeyer-Peppas model

The Korsmeyer-Peppas model is a generalized empirical equation used to characterize different release mechanisms:

$$q_t = k_K t^n \quad (12)$$

where k_K is the release constant and n is the diffusional exponent that determines the release mechanism (Fickian diffusion for $n \leq 0.5$, anomalous for $0.5 < n < 1$). This model is particularly useful for systems with mixed or complex release mechanisms, such as particle disintegration [26].

Thermodynamic analysis

Thermodynamic parameters were derived using the van't Hoff relationship:

$$\ln K = \frac{-\Delta H}{RT} + \frac{\Delta S}{R} \quad (13)$$

where K is the equilibrium constant, derived from the Langmuir model, ΔH is the enthalpy change, ΔS is the entropy change, and ΔG is the Gibbs free energy calculated as $\Delta G = \Delta H - T\Delta S$.

Cytotoxicity assays

The cytotoxicity of functionalized MSNs was evaluated using the 3-[4,5-dimethylthiazol-2-yl]-2,5 diphenyl tetrazolium bromide (MTT; item NO.: M2128, Sigma Aldrich) assay with 3T3 mouse fibroblast cells, kindly donated by a colleague and used in previous studies [27]. Cells were grown in adherent culture flasks containing low-glucose DMEM (item NO.: 31600025, Gibco™) supplemented with 10% heat inactivated fetal bovine serum (item NO.: A56669801, Gibco™) and 1% penicillin-streptomycin (item NO.: A5955, Sigma Aldrich). The samples were kept at 37°C in a humidified 5% carbon dioxide chamber until confluence was reached. Harvesting was performed using trypsin-EDTA solution (item NO.: 15400054, Gibco™). Cells were stained with trypan blue and counted with a Neubauer chamber. Fibroblast cells (8.0×10^4) were seeded in each well of a 24-well plate and added with 1 mL of complete low-glucose DMEM and incubated for 24 h. Cells were then exposed to different MSN concentrations and DexaP-loaded MSNs for 24 h and 48 h. MSN-APTES-DexaP nanoparticles were tested in concentrations of 0.25 mg mL^{-1} and 2.5 mg mL^{-1} . MSN nanoparticles were tested in concentrations of 0.25 mg mL^{-1} and 2.5 mg mL^{-1} . MSN blank consisting of 0.04 mg mL^{-1} . DexaP was also tested. Every assay was done in triplicate. For cell metabolic assessment, the medium was withdrawn and replaced with 50 μL of a 5 mg mL^{-1} MTT solution and 450 μL of cell culture medium and incubated in a humidified 5% carbon dioxide chamber for 4 h. Following incubation, the MTT solution was removed, surfaces were washed three times with phosphate buffered saline (PBS) 1% and 1 mL of absolute ethanol was added. The absorbance was registered at 570 nm using a UV-VIS spectrophotometer (Cecil CE 3021, Cambridge, England) and readings were converted to survival percentage compared to cells with no treatment. In all cases, results are expressed as mean \pm standard deviation (SD) from triplicate experiments [16, 28].

Statistical analysis

Results were expressed as mean values \pm standard error of the mean and represent the mean of 3 independent experiments. Statistical analysis was performed using GraphPad Prism 8.0 (GraphPad Software, Inc.), with a one-way ANOVA followed by Dunnett's test. A significance level of $P < 0.05$ was considered indicative of statistically significant differences. All figures were also prepared using GraphPad Prism 8.0.

Results

Morphological and structural characterization of functionalized MSNs

The morphology of MSNs was evaluated using SEM, TEM, and DLS techniques. SEM images revealed predominantly spherical nanoparticles, while TEM confirmed nanoporous structures with uniform pore distribution. The average hydrated particle size was approximately 666 nm, as measured by DLS, aligning with values reported in similar studies. For instance, Kaasalainen et al. [29] reported that DLS measurements tend to overestimate particle size compared to TEM due to the formation of hydration layers in aqueous environments, which is critical for drug delivery applications. (Figure 1). The observed size increase in the hydrated state compared to TEM and SEM reflects the particle's interaction with its aqueous environment, emphasizing the role of hydration layers in drug delivery contexts. DSC analysis revealed distinct thermal properties for unfunctionalized and functionalized MSNs. Unfunctionalized MSNs exhibited a broad endothermic peak at 120°C, corresponding to the removal of adsorbed moisture. Functionalized MSNs displayed an additional endothermic peak at 240°C, attributed to the decomposition of amino groups grafted onto the MSN surface (Figure 2) [30].

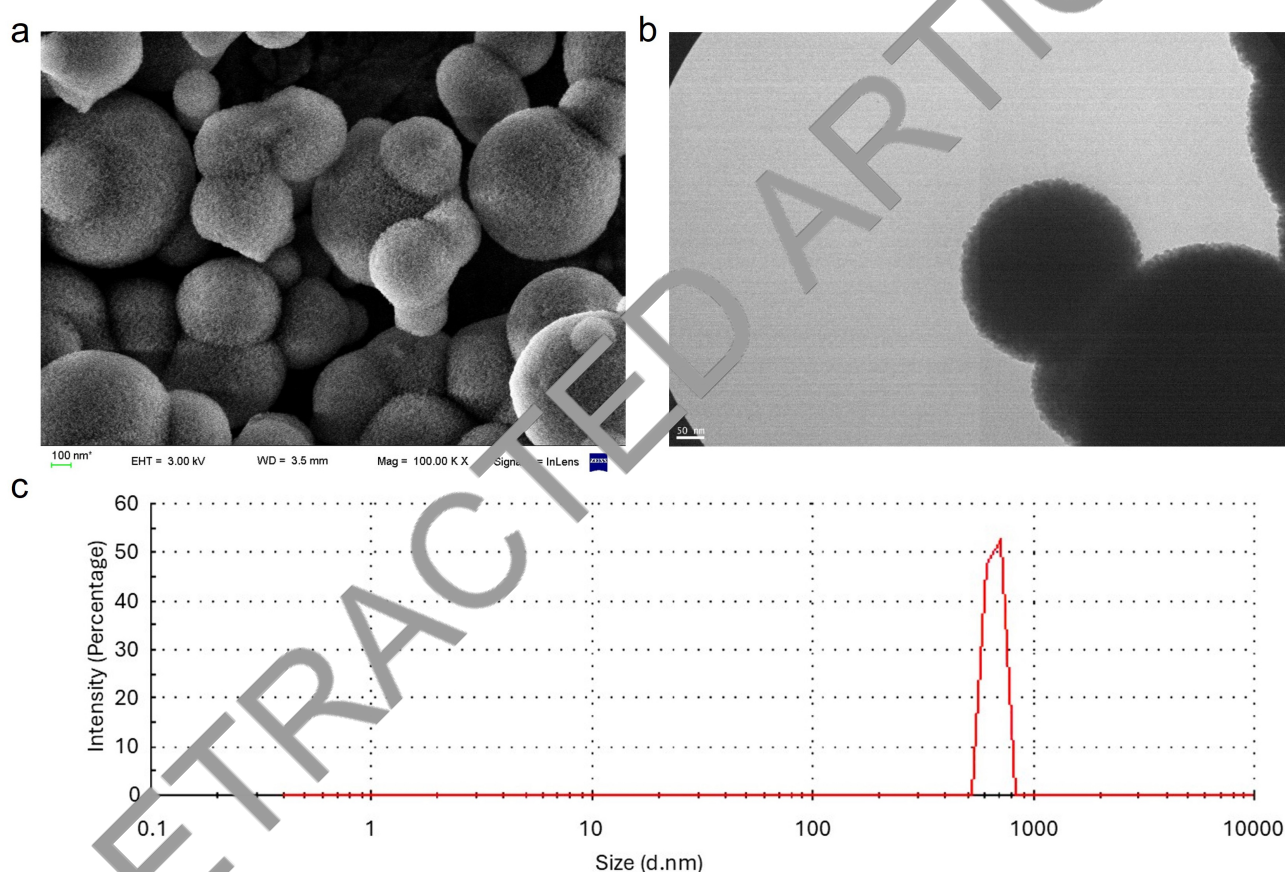


Figure 1. Morphological and structural characterization of functionalized mesoporous silica nanoparticles (MSNs). (a) Scanning electron microscopy images of 3-aminopropyltriethoxysilane (APTES)-modified MSNs displaying a spherical morphology and porous surface structure; (b) transmission electron microscopy images of APTES-modified MSNs highlighting their uniform spherical morphology and well-defined porous structure; (c) dynamic light scattering (DLS) results indicating low particle size dispersion, confirming a monodisperse nanoparticle population

Surface modification and functionalization analysis

Using zeta potential measurements, we confirmed successful functionalization with APTES. At pH 2.0, the zeta potential reached 41.6 mV, indicating positive surface charges from amino groups introduced during functionalization, while at pH 12.0, the potential dropped to -31.6 mV. This pH-dependent surface charge variation aligns with findings by Mebert et al. [10], demonstrating the adaptability of functionalized MSNs in various physiological environments. The strong interaction between the amino groups and DexaP molecules is expected to facilitate a controlled release, especially at neutral and slightly acidic pH levels,

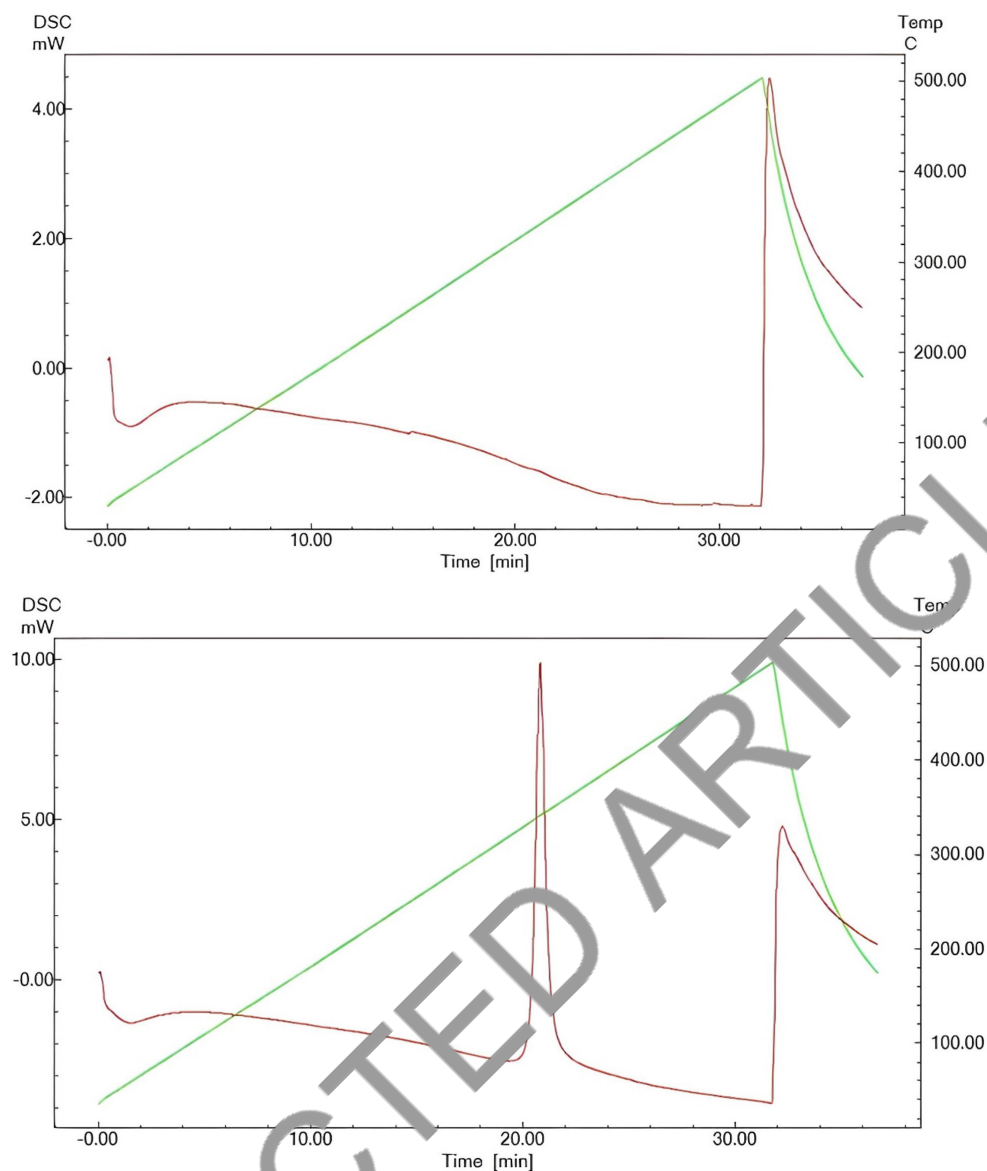


Figure 2. Differential scanning calorimetry (DSC) analysis of mesoporous silica nanoparticles (MSNs). (top) Unfunctionalized MSNs, highlighting the thermal behavior of the unmodified material; (bottom) 3-aminopropyltriethoxysilane (APTES)-functionalized MSNs, showing thermal changes due to surface modification with amino groups. The data provides insights into the thermal stability and structural differences induced by functionalization

ideal for anti-inflammatory applications in bodily tissues. When analyzing the Raman spectra, in both spectra (MSN and APTES-MSN) can be seen two prominent peaks observed at 600 cm^{-1} and $3,250\text{ cm}^{-1}$, attributed to Si-O-Si interactions and free -OH groups, respectively. When the nanoparticles are derivatized with the aminopropyl group, a characteristic peak corresponding to the ethylene ($-\text{CH}_2-\text{CH}_2-$) bond appears at $2,900\text{ cm}^{-1}$, indicating successful attachment. However, no significant decrease in the intensity of the $3,250\text{ cm}^{-1}$ peak is observed, suggesting that the modification with APTES is incomplete (Figure 3) [31].

Adsorption kinetics

When the initial amount of sorbate (DexaP) in solution is high compared to the amount that can be adsorbed by the nanomaterial, the pseudo-first-order model is the best fitting model. On the contrary, when the initial amount of sorbate is comparable with the adsorption capacity of the sorbent (NP), the pseudo-second-order model becomes suitable to fit the data [32]. The results show that the adsorption kinetics fit best with the Elovich model. As mentioned above, this model assumes that the adsorption sites of the sorbent are heterogeneous and therefore exhibit different activation energies for chemisorption, consistent with the findings of Raman spectra.

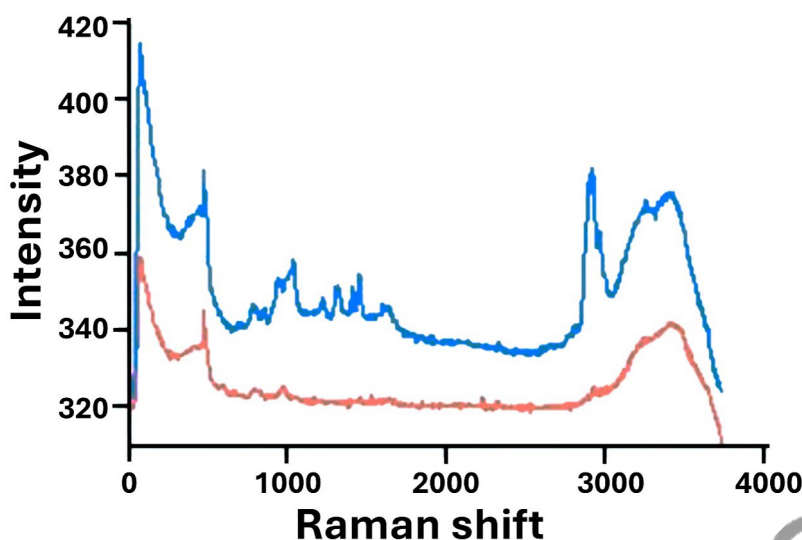


Figure 3. Raman spectra of 3-aminopropyltriethoxysilane (APTES)-functionalized mesoporous silica nanoparticles (APTES-MSN, blue) and non-functionalized MSNs (red). The spectra highlight the functionalization process, showing the characteristic peaks of $-CH_2-CH_2-$ introduced by APTES. Distinct differences between the two spectra emphasize the successful surface modification of the MSNs. Units: Y (AU); X (nm)

Adsorption isotherms

The adsorption behavior of DexaP onto amino-functionalized MSNs was analyzed using Langmuir, Freundlich, D-R, and Temkin isotherms across three temperatures (4°C, 25°C, and 37°C). The Langmuir model provided the best fit at 25°C and 37°C, with $R^2 = 0.9432$ and $R^2 = 0.9617$, respectively, indicating monolayer adsorption with maximum adsorption capacity (q_m) of $0.0045 \pm 0.0002 \text{ mg mg}^{-1}$ at 25°C and $0.0236 \pm 0.0169 \text{ mg mg}^{-1}$ at 37°C, the q_m increased with temperature, consistent with an endothermic process. The Freundlich model also showed a strong correlation at 37°C ($R^2 = 0.9568$), suggesting the continued relevance of heterogeneous surface interactions and multilayer adsorption, particularly at higher temperatures. The D-R isotherm revealed that micropore filling dominated adsorption at lower temperatures ($q_{DR} = 8,882 \pm 801.8 \text{ } \mu\text{mol g}^{-1}$ at 4°C, $R^2 = 0.7762$), with a transition toward macropore adsorption at 37°C ($R^2 = 0.6103$). The Temkin model supported these findings, highlighting adsorbate-adsorbent interactions with a gradual decrease in adsorption energy as surface coverage increased, particularly at lower temperatures ($b = 268.9 \pm 123.5 \text{ J mol}^{-1}$ at 4°C). Table 1 summarizes the results of the fitted models. Together, the isotherm analysis demonstrates that adsorption at physiological temperatures is primarily governed by monolayer adsorption with reduced heterogeneity and increasing adsorption energy, consistent with an endothermic process. The interplay of these mechanisms across temperatures underscores the adaptability of amino-functionalized MSNs for efficient drug loading and controlled release applications.

Table 1. Adsorption parameters and results for adsorption isotherm models

Model	Parameter	4°C	25°C	37°C
Langmuir	$q_m \text{ (mg mg}^{-1}\text{)}$	$0.0043 \pm 0.0004 \text{ (} R^2 = 0.7863\text{)}$	$0.0045 \pm 0.0002 \text{ (} R^2 = 0.9432\text{)}$	$0.0236 \pm 0.0169 \text{ (} R^2 = 0.9617\text{)}$
	$K_a \text{ (L mmol}^{-1}\text{)}$	0.0314 ± 0.0126	0.1013 ± 0.0115	0.8702 ± 0.7818
Freundlich	$K_F \text{ (L g}^{-1}\text{)}$	0.0064 ± 0.0010	0.0047 ± 0.0002	0.0195 ± 0.0036
	n	0.3652 ± 0.0824	0.3615 ± 0.0258	0.9347 ± 0.1200
Dubinin-Radushkevich	$q_{DR} \text{ (}\mu\text{mol g}^{-1}\text{)}$	$8,882 \pm 801.8$	$8,236 \pm 210.0$	$12,613 \pm 2,553.0$
	$K_{DR} \text{ (mol}^2 \text{ k}^{-1} \text{ J}^{-2}\text{)}$	0.0113 ± 0.0025	0.0184 ± 0.0011	0.0256 ± 0.0089
Temkin	$K_T \text{ (mL mg}^{-1}\text{)}$	$1,782 \pm 253.6$	$1,555 \pm 79.4$	$2,400 \pm 400.1$
	$b \text{ (J mol}^{-1}\text{)}$	268.9 ± 123.5	178.5 ± 31.0	112.0 ± 44.4

q_m : maximum adsorption capacity; K_a : Langmuir constant; K_F : adsorption capacity constant; n : heterogeneity factor; q_{DR} : Dubinin-Radushkevich maximum adsorption capacity; K_{DR} : Dubinin-Radushkevich isotherm constant; K_T : equilibrium binding constant; b : Temkin constant

Release kinetics and mechanisms

The kinetics of DexaP release from MSNs were evaluated using zero order, first order, Higuchi, and Korsmeyer-Peppas models, and the results are depicted in Table 2. The Higuchi model exhibited the strongest correlation ($R^2 = 0.9642$), confirming diffusion-controlled release as the dominant mechanism under physiological conditions. The release exponent (n) from the Korsmeyer-Peppas model indicated Fickian diffusion at lower temperatures ($n = 0.46$) and anomalous transport at 37°C ($n = 0.68$), reflecting the combined effects of diffusion and desorption. Temperature-dependent desorption parameters revealed that increasing temperature enhanced molecular mobility and shifted the mechanism toward faster, diffusion-dominated release, consistent with an endothermic process. These findings highlight the adaptability of MSNs for controlled drug release, balancing diffusion and surface interactions based on environmental conditions.

Table 2. Kinetic parameters and results for DexaP desorption models from MSN

Model	Parameter	4°C	25°C	37°C
Zero order	k_0 (mg h ⁻¹)	0.45 ± 0.05	0.63 ± 0.06	0.85 ± 0.08
First order	k_1 (h ⁻¹)	0.22 ± 0.02	0.30 ± 0.02	0.41 ± 0.04
Higuchi	k_H (mg h ^{-1/2})	2.45 ± 0.20	3.12 ± 0.25	4.01 ± 0.30
Korsmeyer-Peppas	n	0.46 ± 0.02	0.54 ± 0.03	0.68 ± 0.04

DexaP: dexamethasone phosphate; MSN: mesoporous silica nanoparticle; k_0 : zero order release constant; k_1 : first-order release constant; k_H : Higuchi constant; n : diffusional exponent

Cytotoxicity evaluation

To assess the biocompatibility of DexaP-loaded MSNs, an MTT assay was performed using 3T3 fibroblast cells. After 24 h, cell viability exceeded 95%, indicating that the nanoparticles had minimal cytotoxicity at this time point. However, at 48 h, a slight decrease in cell viability was observed, which may result from DexaP release or residual particle effects on cellular function. These results are consistent with findings from [10, 28], where similarly functionalized MSNs demonstrated favorable biocompatibility across a range of cell types, underscoring the viability of these particles as drug carriers (Figure 4).

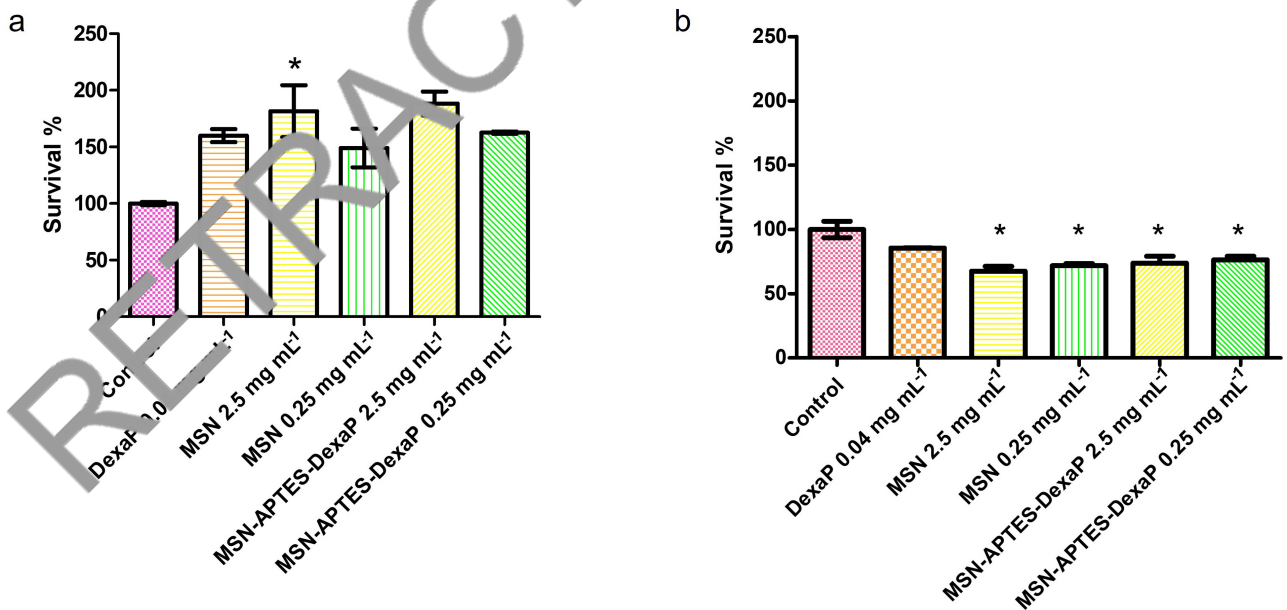


Figure 4. Cytocompatibility assay of mesoporous silica nanoparticles (MSNs) on 3T3 fibroblast cells after 24 h (a) and 48 h (b) of incubation. The assay evaluates the survival percentage of 3T3 cells exposed to various treatments, including the control, free dexamethasone phosphate (DexaP), unmodified MSNs, and 3-aminopropyltriethoxysilane (APTES)-functionalized MSNs loaded with DexaP at different concentrations (2.5 mg mL⁻¹ and 0.25 mg mL⁻¹). Results are expressed as mean ± standard deviation (SD) from triplicate runs. *: $P < 0.05$

Discussion

Recent research has investigated various nanocarriers for drug delivery, including liposomes, polymeric nanoparticles, and non-mesoporous Stöber silica particles, each with unique advantages and limitations. Non-mesoporous Stöber particles, synthesized through the Stöber process, lack internal porosity, resulting in lower drug-loading capacity and less control over release profiles compared to MSNs. These solid silica structures rely on external surface adsorption, which limits functionalization and restricts their application in controlled drug delivery systems. In contrast, MSNs offer tunable pore sizes, high surface areas, and functionalizable internal surfaces, enabling higher drug-loading efficiency and prolonged, controlled release. Compared to polymeric nanoparticles, MSNs exhibit superior stability in physiological conditions and avoid burst release effects commonly observed with polymer-based systems. Similarly, MSNs surpass liposomes, which are prone to degradation and structural instability in biological environments, by maintaining their integrity under physiological conditions, making them suitable for sustained drug delivery. This analysis highlights the versatility and reliability of MSNs as drug delivery platforms, balancing drug-loading efficiency, release control, and adaptability for diverse therapeutic applications, where non-mesoporous Stöber particles and other nanocarriers may fall short.

The results of this study demonstrate the significant potential of MSNs as a platform for the controlled release of DexaP. The nanoparticles exhibited a combination of desirable characteristics, including high adsorption capacity, tunable release profiles, and robust temperature-dependent adaptability, making them suitable for drug delivery applications under varying physiological conditions.

The Langmuir isotherm analysis confirmed efficient monolayer adsorption at physiological temperatures, with a q_m of $0.0236 \text{ mg mg}^{-1}$ at 37°C , underscoring the nanoparticles' ability to load therapeutic quantities of DexaP. The Freundlich model highlighted surface heterogeneity, allowing for effective drug binding across different affinity sites, while the D-R and Temkin models revealed that physical adsorption and moderate adsorbate-adsorbent interactions dominate the process.

Kinetic studies showed that the pseudo-second-order model best described the DexaP uptake, with significant contributions from chemisorptive interactions between the drug and functionalized surfaces. When studying the release of DexaP, the Higuchi and Korsmeyer-Peppas models further demonstrated that diffusion through the porous matrix was the primary mechanism of release, particularly at 37°C , where the diffusion-controlled release was optimized for sustained delivery. The temperature-dependent analysis confirmed that these nanoparticles exhibit an endothermic release process, with enhanced molecular mobility at higher temperatures leading to faster release rates.

The versatility of MSNs is a key feature, as they balance adsorption and diffusion mechanisms to achieve precise release profiles. The ability to modify surface properties through functionalization enables customization for specific drug delivery requirements, including controlled dosing and targeting. Furthermore, the stability and adaptability of MSNs across different environmental conditions enhance their potential for practical biomedical applications.

One of the main contributions of this research is the incorporation of amino groups via APTES, which introduced positive surface charges that improved the interaction with negatively charged DexaP molecules, aligning with similar studies that have demonstrated the benefits of amino-functionalized surfaces for drug adsorption. Unlike conventional MSN systems, where drug release is often limited by rapid diffusion from the outer surface, the MSNs exhibited in this study feature a biphasic release profile that maintained sustained drug levels over an extended period, ideal for conditions requiring prolonged anti-inflammatory effects. This two-phase release, characterized by an initial burst followed by a slower, steady phase, differs from the linear release patterns observed in many other nanoparticle-based systems, which can lead to suboptimal therapeutic windows.

Compared to other nanoparticle platforms, such as polymeric nanoparticles and liposomes, MSNs offer distinct advantages in terms of stability and tunability. Polymeric nanoparticles, while effective for hydrophobic drug delivery, often suffer from stability issues in physiological environments due to their

susceptibility to enzymatic degradation. Liposomes, on the other hand, are prone to rapid clearance by the immune system, necessitating modifications that can compromise their structural integrity. In contrast, MSNs remain structurally stable, even in diverse physiological conditions, due to their inorganic silica matrix, providing a robust carrier with minimal risk of premature degradation. This stability enhances their applicability for systemic and targeted drug delivery, particularly for drugs with stringent dosing requirements, like DexaP.

This study also emphasizes the biocompatibility of amino-functionalized MSNs, validated through cytotoxicity assays with 3T3 mouse fibroblast cells. While some nanoparticle systems have shown moderate to high cytotoxic effects, particularly at higher doses or prolonged exposures, the functionalized MSNs in this study exhibited minimal cytotoxicity, supporting their safe use in therapeutic applications. This finding aligns with Mebert et al. [10], who reported high cell viability in similar biocompatibility assays with functionalized silica nanoparticles, further demonstrating the safety of MSNs as drug carriers. Moreover, the excellent biocompatibility observed in this study underscores the potential of functionalized MSNs not only for drug delivery but also as scaffolding materials in tissue engineering, where minimal cytotoxicity is critical for supporting cell adhesion, proliferation, and tissue regeneration.

Additionally, this research offers insights into the role of surface modification in achieving higher adsorption efficiency and greater release control, advancing beyond the results of previous studies. The combination of particle stability, biocompatibility, and sustained release kinetics makes this approach particularly attractive for developing advanced drug delivery platforms that can support long-term therapeutic interventions with fewer side effects.

Future studies may benefit from exploring *in vivo* models to validate these findings further and optimize the functionalization techniques for even more targeted and personalized drug delivery. Overall, this work contributes a valuable framework for the development of next-generation drug delivery systems, bridging the gap between nanotechnology and precision medicine.

Abbreviations

APTES: 3-aminopropyltriethoxysilane

DexaP: dexamethasone phosphate

DLS: dynamic light scattering

D-R: Dubinin-Radushkevich

DSC: differential scanning calorimetry

MSNs: mesoporous silica nanoparticles

MTT: 3-[4,5-dimethylthiazol-2-yl]-2,5 diphenyl tetrazolium bromide

q_m : maximum adsorption capacity

SEM: scanning electron microscope

TEM: transmission electron microscope

Declarations

Acknowledgments

The authors express their sincere gratitude to Dr. Gisela S. Alvarez for generously providing the 3T3 mouse fibroblast cells, to Dr. Guillermo J. Copello for his invaluable assistance with the interpretation of isotherms and kinetic data, and to Dr. Andrea M. Mebert and Dr. Rodrigo N. Nuñez for their thoughtful revisions and contributions to the final version of the manuscript.

Author contributions

JMG: Conceptualization, Data curation, Formal analysis, Investigation, Methodology, Software, Validation, Visualization, Writing—original draft, Writing—review & editing. MVO: Formal analysis, Investigation,

Methodology, Software, Writing—original draft. AI, DHF, and CMMQ: Investigation, Writing—original draft, Writing—review & editing. MFD: Resources. HP: Data curation, Formal analysis, Investigation, Methodology, Resources, Software, Validation. MVT: Conceptualization, Data curation, Formal analysis, Funding acquisition, Investigation, Methodology, Project administration, Resources, Software, Supervision, Validation, Visualization, Writing—original draft, Writing—review & editing. All authors read and approved the submitted version.

Conflicts of interest

The authors declare that they have no conflicts of interest.

Ethical approval

Not applicable.

Consent to participate

Not applicable.

Consent to publication

Not applicable.

Availability of data and materials

The raw data supporting the conclusions of this manuscript will be made available by the authors, without undue reservation, to any qualified researcher.

Funding

CMMQ is grateful for her doctoral fellowship granted by Universidad de Buenos Aires [RESCD-2024-639-E-UBA-DCT]. This study received grants from the Universidad de Buenos Aires [UBACYT 20020220400378BA, UBACYT 20020190200093BA] and from Agencia Nacional de Investigaciones Científicas y Técnicas [PICT 2018-4154] to MVT. The funders had no role in study design, data collection and analysis, decision to publish, or preparation of the manuscript.

Copyright

© The Author(s) 2025.

Publisher's note

Open Exploration maintains a neutral stance on jurisdictional claims in published institutional affiliations and maps. All opinions expressed in this article are the personal views of the author(s) and do not represent the stance of the editorial team or the publisher.

References

1. Eike IC, Okpala US, Onoja UL, Nwike CP, Ezeako EC, Okpara OJ, et al. Advances in drug delivery systems, challenges and future directions. *Heliyon*. 2023;9:e17488. [DOI] [PubMed] [PMC]
2. Liu K, Mo Q, Ding Z, Lai S, Ren J, Yu Q. Nano theranostics involved in bladder cancer treatment. *Explor Drug Sci*. 2023;1:81–106. [DOI]
3. Xu B, Li S, Shi R, Liu H. Multifunctional mesoporous silica nanoparticles for biomedical applications. *Signal Transduct Target Ther*. 2023;8:435. [DOI] [PubMed] [PMC]
4. Djayanti K, Maharjan P, Cho KH, Jeong S, Kim MS, Shin MC, et al. Mesoporous Silica Nanoparticles as a Potential Nanoplatform: Therapeutic Applications and Considerations. *Int J Mol Sci*. 2023;24:6349. [DOI] [PubMed] [PMC]

5. Salt AN, Hartsock JJ, Piu F, Hou J. Dexamethasone and Dexamethasone Phosphate Entry into Perilymph Compared for Middle Ear Applications in Guinea Pigs. *Audiol Neurotol*. 2018;23:245–57. [DOI] [PubMed] [PMC]
6. Noreen S, Maqbool I, Madni A. Dexamethasone: Therapeutic potential, risks, and future projection during COVID-19 pandemic. *Eur J Pharmacol*. 2021;894:173854. [DOI] [PubMed] [PMC]
7. Kim SJ, Choi Y, Min KT, Hong S. Dexamethasone-Loaded Radially Mesoporous Silica Nanoparticles for Sustained Anti-Inflammatory Effects in Rheumatoid Arthritis. *Pharmaceutics*. 2022;14:985. [DOI] [PubMed] [PMC]
8. Manzano M, Colilla M, Vallet-Regí M. Drug delivery from ordered mesoporous matrices. *Expert Opin Drug Deliv*. 2009;6:1383–400. [DOI] [PubMed]
9. Tuttolomondo MV, Villanueva ME, Alvarez GS, Desimone MF, Díaz LE. Preparation of sub-micrometer monodispersed magnetic silica particles using a novel water in oil microemulsion: properties and application for enzyme immobilization. *Biotechnol Lett*. 2013;35:1571–7. [DOI] [PubMed]
10. Mebert AM, Aimé C, Alvarez GS, Shi Y, Flor SA, Lucangioli SE, et al. Silica core-shell particles for the dual delivery of gentamicin and rifamycin antibiotics. *J Mater Chem B*. 2016;4:3135–44. [DOI] [PubMed]
11. Kamarudin NHN, Jalil AA, Triwahyono S, Salleh NFM, Karim AA, Mukti AR, et al. Role of 3-aminopropyltriethoxysilane in the preparation of mesoporous silica nanoparticles for ibuprofen delivery: Effect on physicochemical properties. *Microporous Mesoporous Mater*. 2013;180:235–41. [DOI]
12. Castillo RR, Lozano D, Vallet-Regí M. Mesoporous Silica Nanoparticles as Carriers for Therapeutic Biomolecules. *Pharmaceutics*. 2020;12:432. [DOI] [PubMed] [PMC]
13. Hoang Thi TT, Cao VD, Nguyen TNQ, Hoang DT, Nguyen MC, Nguyen DH. Functionalized mesoporous silica nanoparticles and biomedical applications. *Mater Sci Eng C*. 2019;99:631–56. [DOI] [PubMed]
14. Kolimi P, Narala S, Youssef AAA, Nyavanandi D, Kundhapa N. A systemic review on development of mesoporous nanoparticles as a vehicle for transdermal drug delivery. *Nanotheranostics*. 2023;7:70–89. [DOI] [PubMed] [PMC]
15. Lérida-Viso A, Estepa-Fernández A, García-Fernández A, Martí-Centelles V, Martínez-Máñez R. Biosafety of mesoporous silica nanoparticles; towards clinical translation. *Adv Drug Deliv Rev*. 2023;201:115049. [DOI] [PubMed]
16. Mebert AM, Evelson P, Desimone MF, Maysinger D. Human lung cell cytotoxicity of antibacterial-loaded silica nanoparticles. *J Drug Delivery Sci Technol*. 2024;92:105298. [DOI]
17. Tuttolomondo MV, Valdepórpura JM, Trichet L, Voisin H, Coradin T, Desimone MF. Dye-collagen interactions: Mechanism, kinetic and thermodynamic analysis. *RSC Adv*. 2015;5:57395–405. [DOI]
18. Ho YS, McKay G. Pseudo-second order model for sorption processes. *Process Biochem*. 1999;34:451–65. [DOI]
19. Langmuir I. THE ADSORPTION OF GASES ON PLANE SURFACES OF GLASS, MICA AND PLATINUM. *J Am Chem Soc*. 1918;40:1361–403. [DOI]
20. Freundlich H. Über die Adsorption in Lösungen. *Z Phys Chem*. 1907;57U:385–470. German. [DOI]
21. Hu Q, Zhang Z. Application of Dubinin–Radushkevich isotherm model at the solid/solution interface: A theoretical analysis. *J Mol Liq*. 2019;277:646–8. [DOI]
22. Dada AO, Lekan AP, Olatunya AM, Dada O. Langmuir, Freundlich, Temkin and Dubinin–Radushkevich Isotherms Studies of Equilibrium Sorption of Zn²⁺ Unto Phosphoric Acid Modified Rice Husk. *IOSR J Appl Chem*. 2012;3:38–45. [DOI]
23. Askarizadeh M, Esfandiari N, Honarvar B, Sajadian SA, Azdarpour A. Kinetic Modeling to Explain the Release of Medicine from Drug Delivery Systems. *CBEN*. 2023;10:1006–49. [DOI]

24. Wojcik-Pastuszka D, Krzak J, Macikowski B, Berkowski R, Osiński B, Musiał W. Evaluation of the Release Kinetics of a Pharmacologically Active Substance from Model Intra-Articular Implants Replacing the Cruciate Ligaments of the Knee. *Materials (Basel)*. 2019;12:1202. [DOI] [PubMed] [PMC]
25. Higuchi WI. Diffusional Models Useful in Biopharmaceutics: Drug Release Rate Processes. *J Pharm Sci*. 1967;56:315–24. [DOI]
26. Korsmeyer RW, Gurny R, Doelker E, Buri P, Peppas NA. Mechanisms of solute release from porous hydrophilic polymers. *Int J Pharm*. 1983;15:25–35. [DOI]
27. Alvarez Echazú MI, Renou SJ, Alvarez GS, Desimone MF, Olmedo DG. Synthesis and Evaluation of a Chitosan–Silica-Based Bone Substitute for Tissue Engineering. *Int J Mol Sci*. 2022;23:13279. [DOI] [PubMed] [PMC]
28. Galdopórpora JM, Ibar A, Tuttolomondo MV, Desimone MF. Dual-effect core–shell polyphenol coated silver nanoparticles for tissue engineering. *Nano-Struct Nano-Objects*. 2021;26:100711. [DOI]
29. Kaasalainen M, Aseyev V, von Haartman E, Karaman DŞ, Mäkilä E, Tenhu H, et al. Size, Stability, and Porosity of Mesoporous Nanoparticles Characterized with Light Scattering. *Nanoscale Res Lett*. 2017;12:74. [DOI] [PubMed] [PMC]
30. Shen SC, Ng WK, Chia L, Dong YC, Tan RBH. Sonoelectrochemical synthesis of (3-aminopropyl)triethoxysilane-modified monodispersed silica nanoparticles for protein immobilization. *Mater Res Bull*. 2011;46:1665–9. [DOI]
31. Hiraoui M, Guendouz M, Lorrain N, Moadhen A, Haji L, Oueslati M. Spectroscopy studies of functionalized oxidized porous silicon surface for biosensing applications. *Mater Chem Phys*. 2011;128:151–6. [DOI]
32. Salazar Camacho CA, Villalobos Peñalosa M. CHARACTERIZATION AND SURFACE REACTIVITY OF NATURAL AND SYNTHETIC MAGNETITES: II. ADSORPTION OF Pb(II) AND Zn(II). *Rev Int Contam Ambient*. 2017;33:165–76. [DOI]